Monthly extreme rainfall risk envelope graph method development and application in Algeria

Sara Zeroual, Zekâi Şen, Hamouda Boutaghane and Mahmoud Hasbaia

ABSTRACT

Rainfall patterns are bound to change as a result of global warming and climate change impacts. Rainfall events are dependent on geographic location, geomorphology, coastal area closeness and general circulation air movements. Accordingly, there are increases and decreases at different meteorology station time-series records leading to extreme events such as droughts and floods. This paper suggests a methodology in terms of envelope curves for monthly extreme rainfall event occurrences at a set of risk levels or return periods that may trigger the extreme occurrences at meteorology station catchments. Generally, in many regions, individual storm rainfall records are not available for intensity–duration–frequency (IDF) curve construction. The main purpose of this paper is, in the absence of individual storm rainfall records, to suggest monthly envelope curves, which provide a relationship between return period and monthly extreme rainfall values. The first step is to identify each monthly extreme rainfall records probability distribution function (PDF) for risk level and return period calculations. Subsequently, the return period rainfall amount relationships are presented on double-logarithmic graphs with the best power model as a set of envelope curves. The applications of these methodologies are implemented for three Hodna drainage basin meteorology station rainfall records in northern Algeria. It is concluded that the most extreme rainfall risk months are June, August and September, which may lead to floods or flash floods in the study area. A new concept is presented for the possible extreme value triggering months through the envelope curves as 'low', 'medium' and 'high' class potentials.

Key words | Algeria, envelope, extreme rainfall, probability, return period, risk

Sara Zeroual (corresponding author)
Mahmoud Hasbaia
VESDD Laboratory,
University of M'sila,
M'sila,
Algeria
E-mail: *zeroual.sara@univ-msila.dz*

Zekâi Şen
Engineering and Natural Sciences Faculty,
Istanbul Medipol University,
Beykoz, 34181 Istanbul,
Turkey
and
Center of Excellence for Climate Change Research/ Department of Meteorology,
King Abdulaziz University,
P.O. Box 80234, Jeddah 21589,
Saudi Arabia

Hamouda Boutaghane
Hydraulics Department, Engineering Faculty,
Badji Mokhtar University,
P.O. Box 12, Annaba,
Algeria

HIGHLIGHTS

- A new methodology is proposed as 'envelope curves' for monthly maximum daily extreme rainfall assessment depending on a set of risk levels or return periods.
- In cases of intensity–duration–frequency (IDF) curves absence, envelope curves can be used to estimate the extreme rainfall events.
- The application of the methodology is given for some Algerian meteorology station rainfall amounts leading to convenient PDF.

INTRODUCTION

Water resources are among the most precious commodities for the socio-economical sustainability of any country, and therefore all over the world effective assessment of their protection against the climate change impacts are advised by scientific and technological means (Cook 2017). Anthropogenic activities in modern life trigger not only air and water pollution, but more alarmingly atmospheric pollution especially due to the greenhouse gas (GHG) emissions,

doi: 10.2166/wcc.2020.176

which initiated the discussion on global warming and consequent climate change impacts on energy, economy and environment, in general, and societal sustainability. In this context, the Intergovernmental Panel on Climate Change reports (IPCC 2007, 2013, 2014) are for general guidance all over the world. It is indicated that an increase in the extreme precipitation risk during the 21st century is likely in the Mediterranean areas (Christensen *et al.* 2013) and the same result is emphasized further for the southern Mediterranean countries by Lionello & Scarascia (2020) using the average rainfall intensity and its fraction during intense events.

Over the Mediterranean countries, the extreme precipitation events have caused significant damage in different sectors of the economy, health and the environment. During 1990–2006, the damage and deaths caused by floods in the Mediterranean region totaled 29.14 billion Euros with the largest number of affected persons in Algeria (Llasat *et al.* 2010; Khodayar *et al.* 2015). According to Gaume *et al.* (2016), the primary natural cause of flooding in this region is the short intense rainfall bursts inducing the convection flows in the Mediterranean Sea. Advance knowledge on rainfall extremes would contribute to better flood planning as well as accurate protection designs by means of hydraulic structures such as flood protection channels and storm sewers. For this purpose, it is important to express the magnitude of extreme events by their occurrence frequency using probability distribution functions (PDFs; Alam *et al.* 2018). The application of statistical theory to model the extreme rainfall is required for different regions since the precipitation events are more dependent on topography, coastal area closeness and general circulation air movement.

In Algeria, several studies have been devoted to analyze and identify regional and local changes in the extreme climatic events (Taibi *et al.* 2015; Djerbouai & Souag-Gamane 2016; Korichi *et al.* 2016; Achour *et al.* 2020). Benkhaled (2007) found that the generalized extreme value (GEV) and Gumbel PDFs provide the best fit with almost similar results based on a return period of 100 years for four annual maximum daily rainfall records in the Cheliff-Zahrez basin, northwest Algeria, where Benhattab *et al.* (2014) identified the GEV PDF as the most appropriate regional distribution for annual maximum daily rainfall records, which are characterized by a Mediterranean climate. A comparison between the GEV and Gumbel PDFs on annual maximum daily rainfall was established by Boucefiane *et al.* (2014) at some rain gauge stations located in the steppe region of western Algeria. The authors proved that the Gumbel PDF suggested by the National Hydraulic Resources Agency (ANRH 2007) was not suitable for this region. The GEV and the Generalized Logistics (GLO) PDFs were identified as the most appropriate for modeling annual maximum daily rainfall in northern Algeria (Zeggane & Boutoutaou (2017). Many authors have been interested in frequency distributions of monthly maximum daily rainfall records in several different regions around the world (Şen & Eljadid 1999; Eslamian & Feizi 2007; Bhakar *et al.* 2008; Mandal & Choudhury 2015; Alam *et al.* 2018). Şen & Eljadid (1999) found that in Libyan arid regions (border country of Algeria), the Gamma PDF provided the best fit. In the same way, Amiri & Eslamian (2010) suggested that the GEV and Pearson type-III were suitable for Iranian arid region monthly precipitation records. Currently, most Algerian engineers who applied the annual extreme precipitation data for design purposes used the Gumbel PDF (ANRH 2007), despite the fact that it produces small design rainfall values for large return periods (Koutsoyiannis 2004, 2007; Zahar & Laborde 2007; Shabri & Mohd Arif 2009; Cavicchia *et al.* 2018). Consequently, any engineering water structure design based on such calculations showed improper performances.

Based on the above insights, the overall goal of this study is to identify the PDF for monthly maximum daily rainfall records at a set of three meteorology stations in the Hodna basin, Algeria. A new approach is presented under the name of envelope curves for monthly extreme rainfall assessments. The envelope curve or broken line in a plane subsumes all the alternatives under its umbrella, i.e., it is the maximum boundary of the events depending on the hydro-meteorological variable, which is the monthly extreme precipitation value in this paper.

In case of intensity–duration–frequency (IDF) curve absence in a region, envelope curves provide rainfall amounts based on a set of risk levels and return periods. The envelope curves appear as a straight line on double-logarithmic Cartesian coordinate systems between the extreme monthly rainfall amounts and return periods. The application of the proposed methodology has been performed for three meteorology stations, monthly extreme rainfall records.

STUDY AREA AND METHODOLOGY

In general, the study area and the meteorology station locations that are considered in this study are given in Figure 1. The study area is within the Hodna basin as shown in Figure 2.

In Algeria, the Hodna basin ranks as the fifth biggest and is situated in the center Isser, Soummam, Hauts plateaux, Chott Merlhir, Zahrez and Chelif surrounding basins as shown in Figure 2. The surface area is about 26,000 km^2, and it is between two topographic ensembles of Atlas and African Sahara. It also lies within two mountainous regions with 1,800–1,900 m elevations in the north and 600–900 m in the south.

The surface slope encourages rapid surface flow leading to occasional floods and flash floods. The Honda basin has four different feature geomorphological units as mountainous region, Hodna valley, Chott sabkha and R'mel piedmont regions. Table 1 indicates the geographic locations and basic statistical parameters for the three stations that are considered in this study.

The average precipitation in the Hodna basin at about 400 m elevations is 200 mm, but at higher elevations (about 1,800 m), it reaches 600–700 mm. In winter, snow falls on the Hodna Mountains and remains on the surface for 20–30 days at the maximum.

The temperature degrees vary according to elevation and local conditions. Evaporation is rather high, and due to the effect of wind, the surface water ponds lose water rather rapidly. In the Hodna basin, average maximum temperature changes according to the geographic features. The average annual temperatures are 18 °C in the northwest, 18.5 °C in the center and northeast and 17.9 °C in the south of the basin (Hasbaia *et al.* 2012; Salhi *et al.* 2013).

Geographically, the watershed region is between 3°1′-6°12′E and 34°15′-36°15′N within three different climatic regions (Figure 3), according to Köppen's climate classification, namely the Mediterranean hot summer climates (Csa) in the northern part of the watershed, a belt of cold semi-arid climate (BSk) in the center and desert (BWh) with semi-arid (BSh) climate in the southernmost portion of the watershed (Zeroual *et al.* 2019).

The rainfall map of the Hodna Basin is prepared based on CHIRPS satellite-gauge data at 0.05° resolution over the 2000–2014 period (Funk *et al.* 2015; Figure 3).

The spatial distribution of rainfall is characterized by a strong gradient from the northwest to Chotelhodna, with a less marked South Chotelhodna gradient. The average annual rainfall drops from around 500–600 mm on mountain ridges of the Hodna (region of Bordj Bou Arreridj) to less than 200 mm at Chottelhodna. The average annual rainfall in the southern region ranges between 300 and 390 mm (Boussaada and Ain Rich locations). This high variability is due to the north-south contrast of the basin (Hasbaia *et al.* 2017). The low precipitation values found at the center and south of the basin are due to the remoteness of the region from the Mediterranean Sea and to the mountainous obstacle constituted by the El-Hodna Mountain, which prevent the progression of the moisture-bearing northerly winds. Summer drought is general, but there is also a frequent dry period in winter.

METHODOLOGICAL APPROACH

In general, individual storm rainfall amounts assessment toward IDF curves determination provides flood risk assessment foundations. In semi-arid and arid regions, such storm rainfall records are not available, and therefore, it is necessary to base the flood assessments on daily total rainfall amounts, which are in most cases representative of individual rainfall events. Extreme rainfall amount predictions are among the most significant feature identifications because their consequent results may cause floods and flash floods leading to both human property and loss of life.

In general, extreme values are represented by Gamma PDF functions, which are the case with Algerian rainfall amounts (Achour *et al.* 2020). The three-parameter PDF is also referred to as the Pearson III PDF and its general mathematical expression is given as (Thom 1958; Wilk *et al.* 1962; Bobee 1973; Bobee & Ashkar 1991; Haktanır 1991;

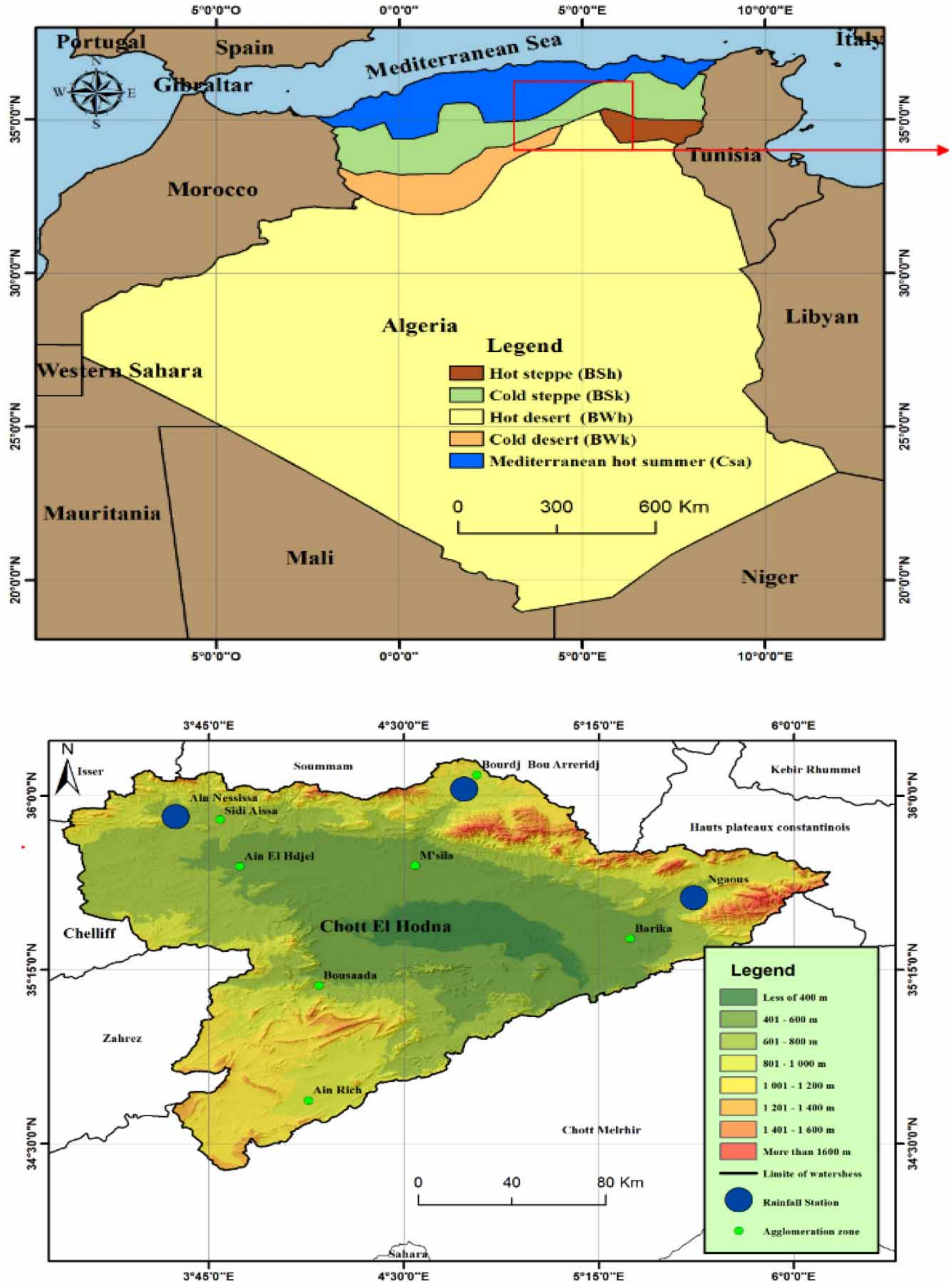

Figure 1 | Study area and station locations.

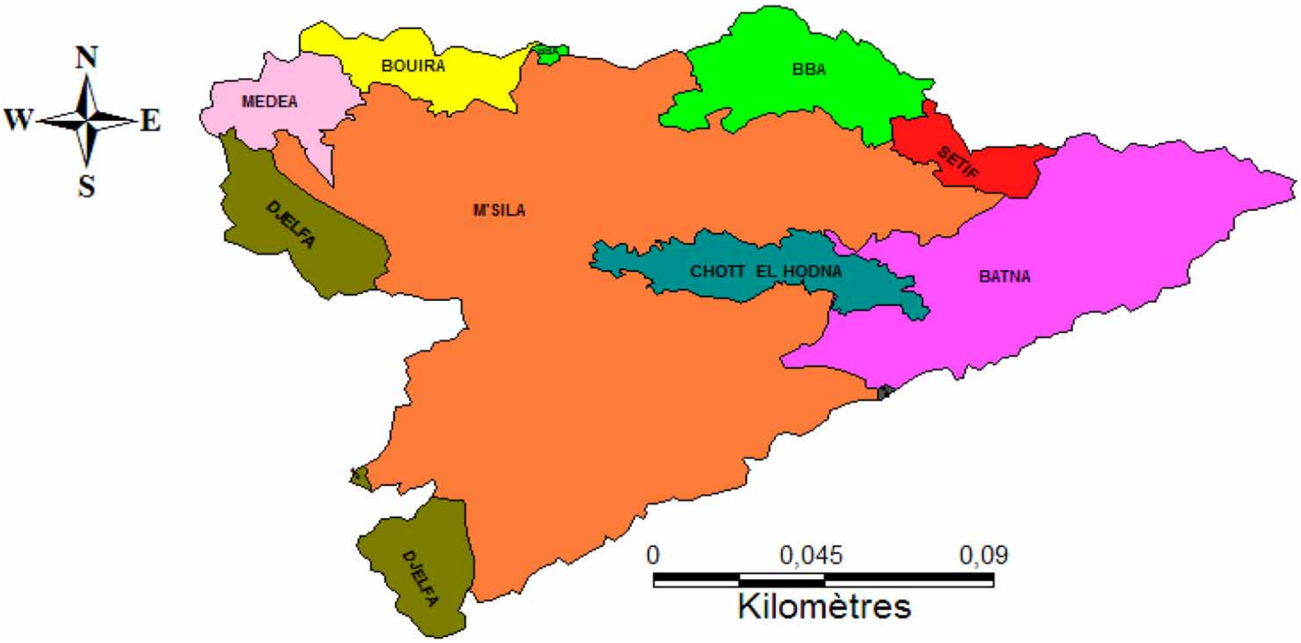

Figure 2 | Hodna basin location.

Table 1 | Names, geographic coordinates, elevation and annual mean precipitation with standard deviation, maximum and minimum for the three stations considered in the study (1968–2013)

Station code	Station name	Longitude (E)	Latitude (N)	Elevation (m)	Mean (mm)	Standard deviation (mm)	Maximum (mm)	Minimum (mm)
50101	Ain Nessissa	4°10′18″	32°52′33″	680	34.59	21.82	132.60	11.60
51306	Ngaous	5°33′6″	32°40′0.91″	750	37.90	18.74	85.40	11.20
50905	BB Arreridi	4°55′38″	33°3′55″	922	32.71	10.20	53.50	15.50

Guttman 1999; Lloyd-Hughes & Saunders 2002)

$$f(x) = \frac{1}{a\Gamma(b)}\left(\frac{x-c}{a}\right)^{b-1} e^{-((x-c)/a)} \quad (1)$$

where $a > 0$, $b > 0$ and $0 < c < x$ are the PDF parameters. These are referred to as the location, scale and shape parameters, respectively. It can be given simpler form by defining that $y = (x - c)/a$, and hence, it takes the following form:

$$f(y) = \frac{1}{\Gamma(b)} y^{b-1} e^{-y} \quad (2)$$

On the other hand, two-parameter Gamma PDF has easier parameter calculations and the mathematical expression has the following form:

$$f(x) = \frac{1}{b^a\Gamma(a)} x^{a-1} e^{-x/b} \quad (3)$$

The PDF matching the available data at each meteorology station is achieved through the execution of the following steps. Let the given annual monthly extreme rainfall records be representative as $X_1, X_2, X_3, \ldots, X_n$, where n is the number of data.

(1) Arrange the given data into ascending order, hence a new non-decreasing sequence is obtained as $Y_1 < Y_2 < Y_3 < \ldots < \ldots < Y_n$ with ranks, m, as 1, 2, 3, …, $m = n$, respectively.
(2) Attach to each value in the ordered sequence a non-exceedence probability value, P_m, according to the

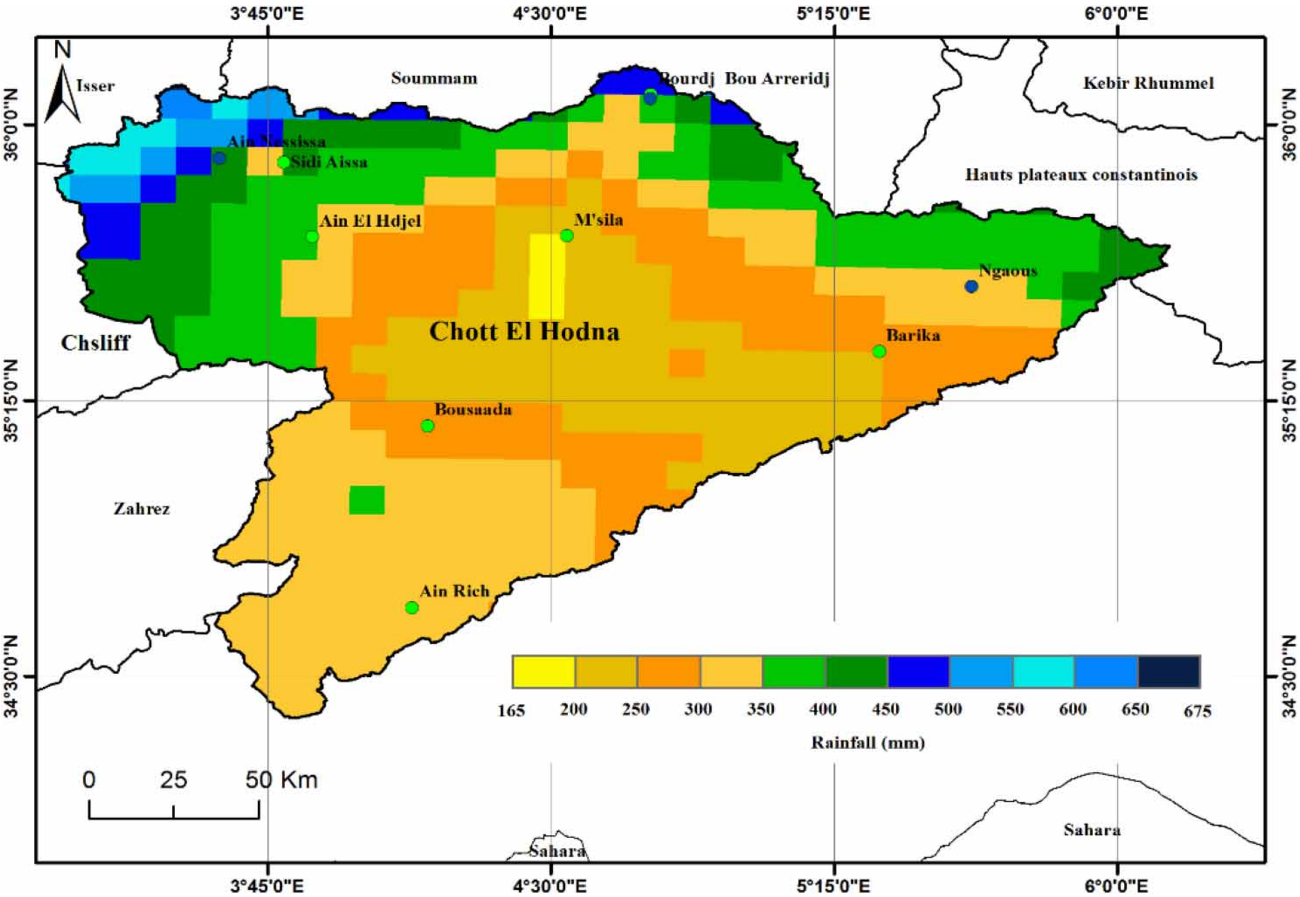

Figure 3 | Annual mean precipitations in HODNA watershed (2000–2014) (CHIRPS at 0.05° × 0.05°).

following empirical formulation:

$$P_m = \frac{m}{n+1} \quad (0 < P_m < 1) \tag{4}$$

(3) Plot the scatter diagram of ordered sequence versus corresponding probability values (Y_m versus P_m). Hence, a non-decreasing systematic scatter diagram appears. Furthermore, if one wants to work with exceedence probabilities, then the scatter diagram takes the form of non-increasing form after plot of Y_m versus $(1 - P_m)$. Hence, empirical systematic probability points scatter appear on the normal paper.

(4) These points are fitted with the best PDF among many alternatives such as normal (Gauss), log-normal, Weibull, two- and three-parameter Gamma (Pearson III) PDFs which is achieved through the MATLAB program software written by Şen (2020).

(5) Finally, the plot of the best fit PDF on the scatter diagram leads to figures with a set of risk levels and also the type and parameters of the best theoretical PDF as explained above in Equations (1)–(3).

One must keep in mind that there is a difference between the probability and risk. The probability is given by Equation (4), whereas the risk depends on decision makers such as 5 and 10%, for design purpose after the identification of the theoretical PDF.

In this study, three meteorology stations are taken into consideration and detailed explanation about the methodological application is written for one of them because the same procedure is used in three of them. Figure 4 presents the results obtained for each month at Ain Nssissa (Station 1) after the application of the previous steps to the

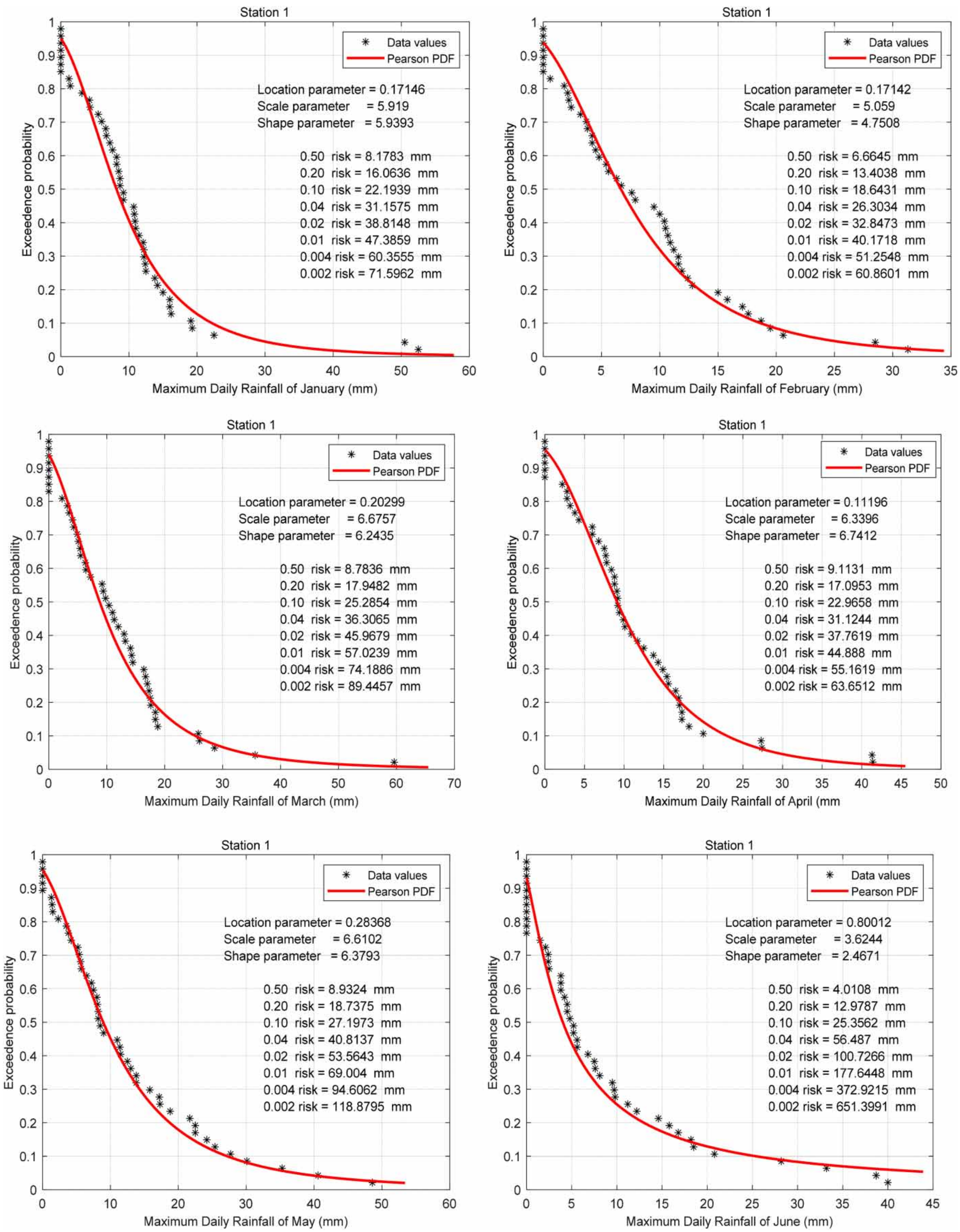

Figure 4 | Risk graphs for each month at Ain Nssissa meteorology station. *(continued).*

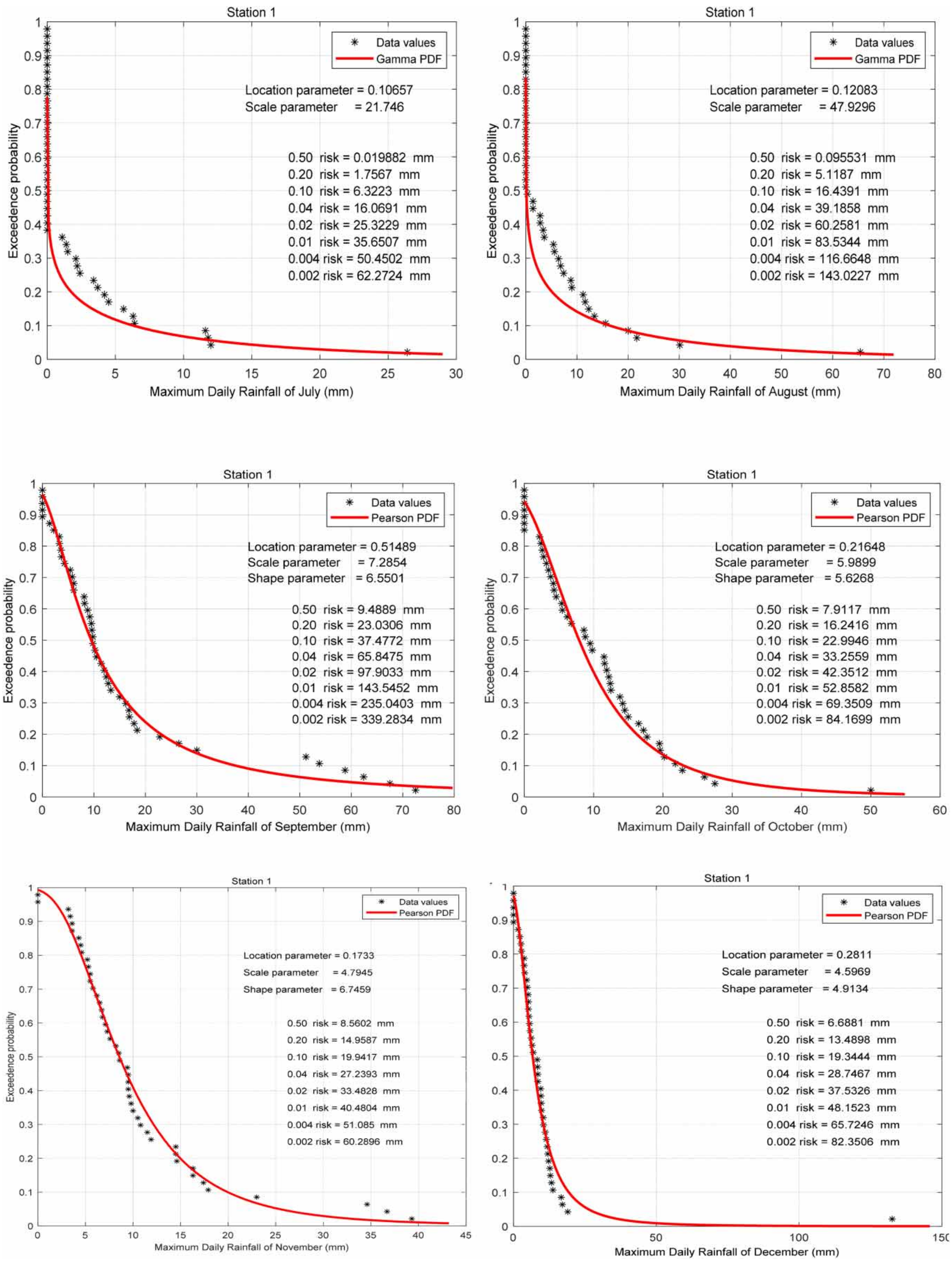

Figure 4 | Continued.

monthly extreme rainfall data. It is obvious that in each month, only two- and three-parameter Gamma PDFs are the most suitable theoretical PDFs.

Table 2 indicates the extreme rainfall events corresponding to a set of risk levels, which also appear in each graph in Figure 4, only for Ain Nssissa meteorology station.

The summary of all that can be inferred from the graphs in Figure 4 is presented in Table 3.

EXTREME RAINFALL RETURN PERIOD GRAPH

In the absence of IDF curves, the relationship between the return periods or risk levels and monthly extreme rainfall values provides a scientific basis for extreme value calculation opportunity leading to graphs, which can be referred to as the risk extreme value diagrams and can be drawn from the values in Table 3 for Ain Nssissa station. The resulting graphs are given in Figure 5 on the double-logarithmic scales.

The mathematical model is a power function with two parameters, a and b, which can be written as:

$$Y = aX^b \quad (5)$$

or as follows

$$\log X = \log a + b \log X \quad (6)$$

where X represents the return period variable on the horizontal axis and Y is for the extreme rainfall amount.

Table 2 | The extreme rainfall risk months

Ain Nssissa station

Return period (year)	Risk (%)	Maximum precipitation (mm)	Month
2	50	24.39	September
5	20	37.16	–
10	10	51.11	–
25	4	77.87	–
50	2	112.29	August
100	1	383.56	June
250	0.4	2,352.23	–
500	0.2	9,274.93	–

Table 3 | Return period, risk and monthly extreme rainfall values (mm)

Return period (Year)	Risk (%)	Jan.	Feb.	Mar.	Apr.	May	Jun.	Jul.	Aug.	Sep.	Oct.	Nov.	Dec.	Min. (mm)	Mean (mm)	Max (mm)	Standard deviation (mm)
2	50	8.18	6.66	8.78	9.11	8.93	4.01	0.02	0.10	9.49	7.91	0.56	6.69	0.02	5.87	9.49	3.71
5	20	16.06	13.40	17.95	17.10	18.74	12.98	1.76	5.12	23.03	16.24	14.96	13.49	1.76	14.24	23.03	5.79
10	10	22.19	18.64	25.29	22.97	27.20	25.36	6.32	16.44	37.48	22.99	19.94	19.34	6.32	22.01	37.48	7.32
25	4	31.16	26.30	36.31	31.12	40.81	56.49	16.07	39.19	65.85	33.26	27.24	28.75	16.07	36.04	65.85	13.55
50	2	38.81	32.85	45.97	37.76	53.56	100.73	25.32	60.26	97.90	42.35	33.48	37.53	25.32	50.54	100.73	24.61
100	1	47.39	40.17	57.02	44.89	69.00	177.64	35.65	83.53	143.55	52.86	40.48	48.15	35.65	70.03	177.64	44.93
250	0.4	60.36	51.25	74.19	55.16	94.61	372.92	50.45	116.66	235.04	69.35	51.09	65.72	50.45	108.07	372.92	98.09
500	0.2	71.60	60.86	89.45	63.65	118.88	651.40	62.27	143.02	339.28	84.17	60.29	82.35	60.29	152.27	651.40	175.31

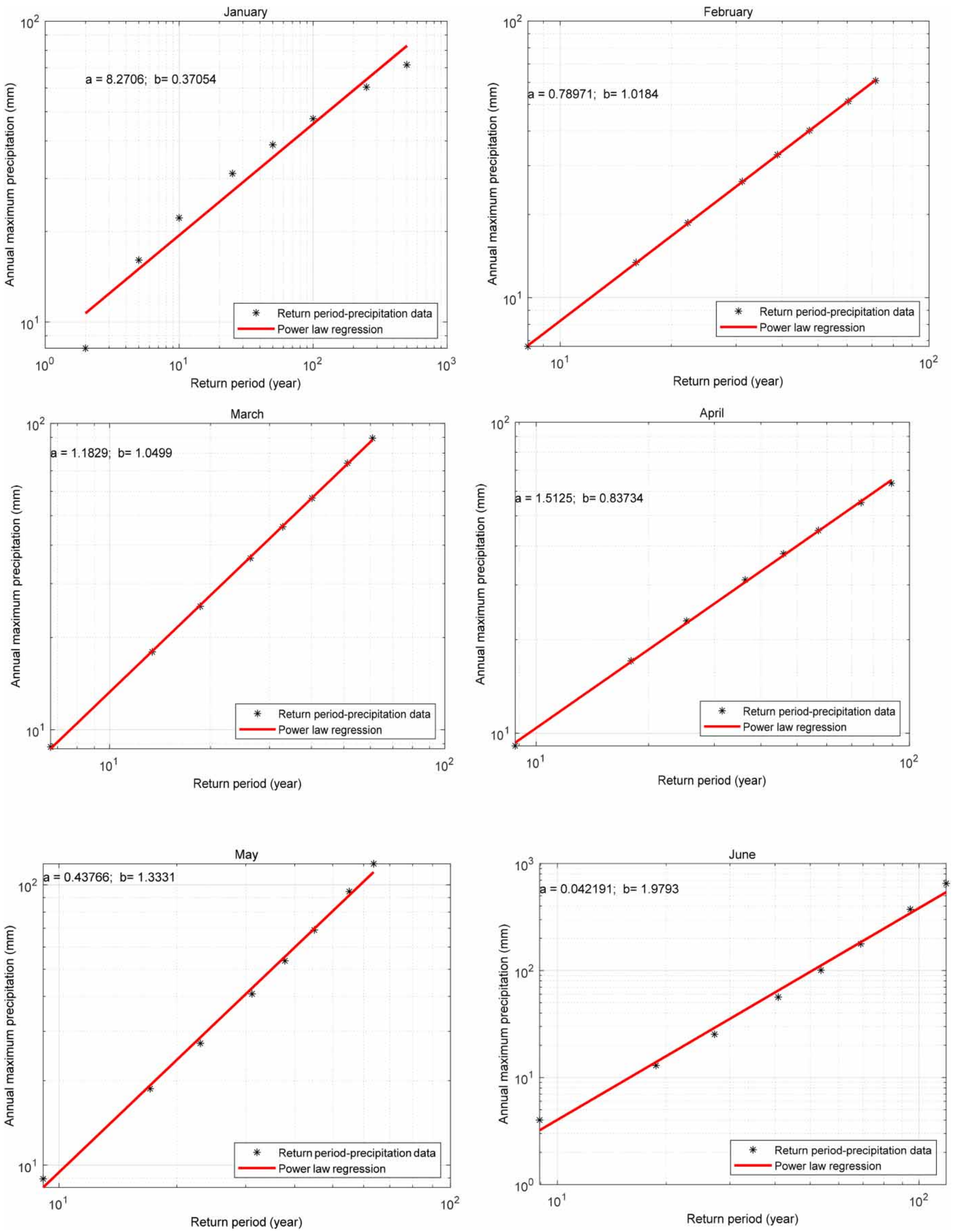

Figure 5 | Return period and extreme rainfall value graphs. Please refer to the online version of this paper to see this figure in colour: http://dx.doi.org/10.2166/wcc.2020.176. *(continued.).*

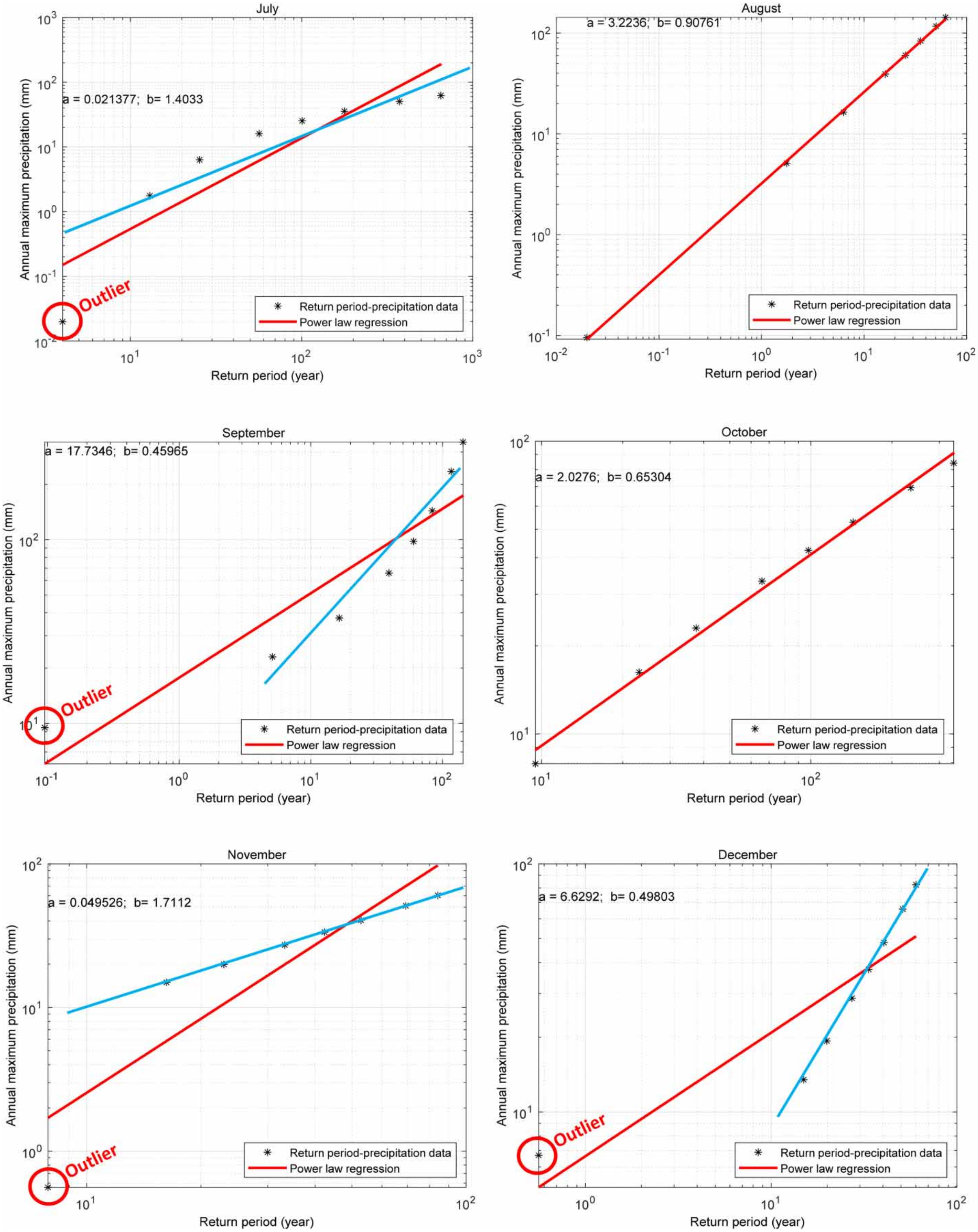

Figure 5 | Continued.

Table 4 | Power law parameters

Months	*a*	*b*
Jan.	8.27	0.37
Feb.	0.79	1.02
Mar.	1.18	1.05
Apr.	1.51	0.84
May	0.44	1.33
Jun.	0.04	1.98
Jul.	0.02	1.40
Aug.	3.22	0.91
Sep.	17.73	0.46
Oct.	2.02	0.65
Nov.	0.05	1.71
Dec.	6.63	0.50
Average	3.49	1.02
Standard deviation	5.00	0.48

In Figure 5, the red straight lines are valid with intercept, *a*, and slope, *b*, values, which are calculated through the application of regression methodology. In cases of outliers, the regression line does not present a completely representative straight line. In Figure 5, the months of July, September, October, November and December have outliers, and therefore, the regression lines without outliers are presented by blue straight lines for these months. Table 4 includes the monthly parameters of power low model parameters.

DISCUSSION

The combination of the information from the two previous sections provides an integrated monthly extreme precipitation and return period relationship as indicated in Figure 6. The first striking fact is an upper envelope boundary for extreme rainfall occurrence possibilities as described by means of 'low', 'medium' and 'high' risk levels. The quantitative rainfall values are presented in Table 5 corresponding to three return periods and risk levels. One can deduce the following significant points from these graphs:

(1) The month with the least precipitation risk is July because its return period values remain almost below each monthly values.
(2) The upper envelope of extreme precipitation occurrence possibility takes place along different months as June, August and September.
(3) The 'high' risk cases are bound to appear in June, where the 100-year return period value corresponds to 380 mm in June. The next 'high' risk extreme rainfall amounts are bound to appear in May and then in November.
(4) The 'medium' risk occurs in August corresponding to a 50-year return period with 110 mm rainfall expectation. The next month in this risk category is transition from June–August to September.
(5) The 'low risk' flood occurrence risk is confined to September for return periods up to 50 years, and for example, the 10-year return period extreme rainfall amount is about 50 mm.
(6) For any given return period in a year, one can classify the months according to their respective values from the top down.
(7) Any given monthly rainfall value can be categorized according to the return period values from the smallest to the biggest.

In Figure 6(a), the Ain Nssissa meteorology station in the west presents extreme rainfall amount change by return period on double-logarithmic paper for each month. It is obvious that the lowest rainfall amounts appear in July, which could be regarded as drought impact occurrence in this month. On the other hand, the envelope broken line has three classes in sequence as 'low' in September, 'medium' in August and 'high' rainfall occurrence expectations in June. The extreme rainfall variations along the upper envelope broken line are less than 110 mm for 'low', between 100 and 130 mm for 'medium' and more than 130 mm for the 'high' extreme rainfall occurrences.

The envelope straight lines on double-logarithmic paper are given for Ngaous meteorology station in Figure 6(b), where the bunch of monthly lines are rather close to each other compared with the previous station, but there appears an off line in June, which has both lower rainfall and along the envelope line high-risk component for extreme rainfall occurrences. This point indicates that this month is for rather 'low' extreme rainfall occurrences in the domain of the dry period. However, it also has the 'high' extreme rainfall occurrence in the upper envelope boundary with more

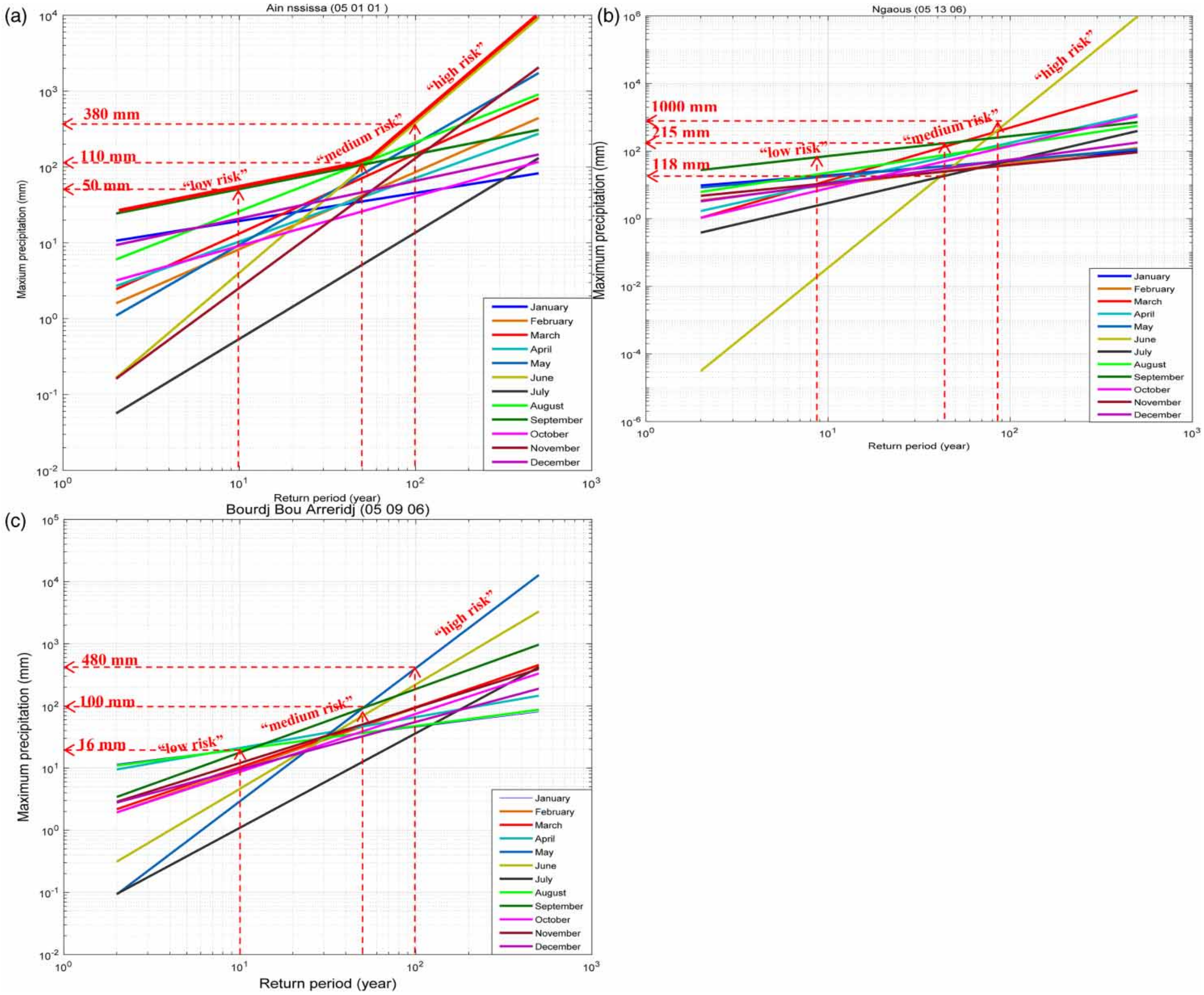

Figure 6 | Monthly extreme rainfall and return period relationships: (a) Ain Nssissa (in the west), (b) Ngaous (in the east) and (c) Bourdji Bou Arreridj (in the south).

Table 5 | Extreme rainfall return periods and amounts

		Meteorology stations		
Classes	**Descriptions**	**Ain Nssissa**	**Ngaous**	**Bourdj Bou Arreridj**
'Low'	Month	July	September	July
	Rainfall range (mm)	< 110 mm	< 215 mm	< 16 mm
'Medium'	Month	August	August	August
	Rainfall range (mm)	110–380 mm	215–1,000 mm	16–100 mm
'High'	Month	June	March	April
	Rainfall range (mm)	> 380 mm	> 1,000 mm	> 100 mm

Table 6 | Monthly envelope values

	Return period and risk		
Station name	**10-year 0.10**	**50-year 0.02**	**100-year 0.01**
AinNessissa	50	110	380
Ngaous	118	215	1,000
BB Arreridj	16	100	480

than 400 mm, which has a very occasional chance of occurring. September plays a dominant role in the 'low' extreme rainfall occurrences with less than 215 mm, whereas a short duration 'medium' extreme rainfall domain has extreme rainfall amounts that may vary from 215 to 400 mm.

Finally, Bourdj Bou Arreridj meteorology station in the south has an overwhelmingly lower extreme rainfall line in July with expected extreme rainfall amounts that vary from 0.1 to almost 200 mm. Along the envelope line, there are three distinctive monthly parts. The 'low' extreme rainfall values are along the August month for about a 15-year return period. September appears for 'medium' extreme rainfall expectations from 16 to 100 mm, and the 'high' part is during April with more than 100 mm extreme rainfall (Table 5).

Finally, Table 6 is prepared for monthly extreme precipitation values for 10-year, 50-year and 100-year return periods with corresponding risk levels of 0.10, 0.20 and 0.01, respectively.

CONCLUSIONS

The main purpose of the paper was to identify first the PDF for each monthly extreme rainfall value to find the return periods (inverse of risk levels), which play a significant role in extreme rainfall frequency analysis. The return period and monthly extreme rainfall value relationship is obtained for each month, which appeared in the form of straight lines on double-logarithmic paper. These double-logarithmic plots expose which months are for extreme rainfall events and the length of the return period. The application of the proposed methodology indicated that the monthly extreme rainfall PDFs have either two- or three-parameter (Pearson III) Gamma mathematical formulations. However, return period and monthly extreme rainfall values are in the form of power function for which parameters are also obtained. A new concept of extreme rainfall envelope is developed and applied for three stations, which provide useful information in the absence of IDF curve absences. The applications of these methodologies are presented for the Hodna drainage basin in Algeria through three meteorology stations' monthly daily maximum rainfall amounts.

REFERENCES

Achour, K., Meddi, M., Zeroual, A., Bouabdelli, S., Maccioni, P. & Moramarco, T. 2020 Spatio-temporal analysis and forecasting of drought in the plains of northwestern Algeria using the standardized precipitation index. *Journal of Earth System Science* **129** (1), 42.

Alam, M. A., Emura, K., Farnham, C. & Yuan, J. 2018 Best-fit probability distributions and return periods for maximum monthly rainfall in Bangladesh. *Climate* **6** (1), 9.

Amiri, M. J. & Eslamian, S. S. 2010 Investigation of climate change in Iran. *Journal of Environmental Science and Technology* **3** (4), 208–216.

ANRH 2007 *Etude de synthèse des crues sur l'Algérie du Nord', Ministère des Ressources en Eau, Algérie/Flood Synthesis Study on Northern Algeria*. Ministry of Water Resources, Algeria, p. 64.

Benhattab, K., Bouvier, C. & Meddi, M. 2014 Analyse fréquentielle régionale des précipitations journalières maximales annuelles dans le bassin hydrographique-Chéliff, Algérie/ Regional frequency analysis of maximal daily annual rainfalls in Cheliff catchment, Algeria. *Revue des sciences de l'eau/ Journal of Water Science* **27** (3), 189–203.

Benkhaled, A. 2007 Distributions statistiques des pluies maximales annuelles dans la région du Cheliff comparaison des techniques et des résultats/Statistical distributions of annual maximum rainfalls depths in the area of Cheliff. comparison of techniques and results. Larys N°08, pp. 83–91.

Bhakar, S. R., Iqbal, M., Devanda, M., Chhajed, N. & Bansal, A. K. 2008 Probability analysis of rainfall at Kota. *Indian Journal of Agricultural Research* **42**, 201–206.

Bobee, B. 1973 Sample error of T-year events computed by fitting a Pearson type-3 distribution. *Water Resources Research* **9** (5), 1264–1270. CrossRefGoogle Scholar.

Bobee, B. & Ashkar, F. 1991 *The Gamma Family and Derived Distributions Applied in Hydrology*. Water Resources Publications, Littleton, CO.

Boucefiane, A., Meddi, M., Laborde, J. P. & Eslamian, S. 2014 Rainfall frequency analysis using extreme values distributions in the steppe region of Western Algeria. *International Journal of Hydrology Science and Technology* **4** (4), 348–367.

Cavicchia, L., Scoccimarro, E., Gualdi, S., Marson, P., Ahrens, B., Berthou, S. & Dubois, C. 2018 Mediterranean extreme precipitation: a multi-model assessment. *Climate Dynamics* **51** (3), 901–913.

Christensen, J. H., Boberg, B., Christensen, O. B. & Lucas-Picher, P. 2013 On the need for bias correction of regional climate change projections of temperature and precipitation. *Geophysical Research Letters* **35**, L20709. doi:10.1029/2008GL035694.

Cook, H. F. 2017 *The Protection and Conservation of Water Resources*. 2nd edn. ISBN:9781119970040.

Djerbouai, S. & Souag-Gamane, D. 2016 Drought forecasting using neural networks, wavelet neural networks, and stochastic models: case of the Algerois basin in North Algeria. *Water Resources Management* **30** (7), 2445–2464.

Eslamian, S. S. & Feizi, H. 2007 Maximum monthly rainfall analysis using L-moments for an arid region in Isfahan Province, Iran. *Journal of Applied Meteorology and Climatology* **46**, 494–503.

Funk, C., Peterson, P., Landsfeld, M., Pedreros, D., Verdin, J., Shukla, S., Husak, G., Rowland, H., Hoell, J., A, L. & Michaelsen, J. 2015 The climate hazards infrared precipitation with stations – a new environmental record for monitoring extremes. *Scientific Data* **8** (2), 150066. https://doi.org/10.1038/sdata.2015.66.

Gaume, E., Borga, M., Llassat, M. C., Maouche, S., Lang, M. & Diakakis, M. 2016 Mediterranean extreme floods and flash floods. The Mediterranean Region under climate change. A Scientific Update, IRD Editions, pp. 133–144, Coll. Synthèses, 978-2-7099-2219-7.

Guttman, N. B. 1999 Accepting the standardized precipitation index: a calculation algorithm. *Journal of the American Water Resources Association* **35**, 311–322.

Haktanir, T. 1991 Practical computation of gamma frequency factors. *Hydrological Sciences Journal* **36** (6), 599–610.

Hasbaia, M., Hedjazi, A. & Benayada, L. 2012 Variabilité de l'érosion hydrique dans le bassin du Hodna: cas du sous-bassin versant de l'oued elham/Variability of erosion in the Hodna basin: case of the Oued Elham watershed. *Revue Marocaine des Sciences Agronomiques et Vétérinaires* **1** (1), 28–32.

Hasbaia, M., Paquier, A. & Herizi, T. 2017 Hydrological modeling of sediment transport in the semi-arid region, case of Soubella watershed in Algeria. In: *Water Resources in Arid Areas: The Way Forward*. (O. A. Abdalla, A. R. Kacimov, M. Chen, A. Al-Maktoumi, T. K. Al Hosni & I. Clark eds.) Springer, Cham, pp. 251–266.

IPCC 2007 *IPCC Fourth Assessment Report Working Group I Report 'The Physical Science Basis'*. Cambridge University Press, New York.

IPCC 2013 *Climate Change 2013: The Physical Science Basis. Contribution of Working Group I to the Fifth Assessment Report of the Intergovernmental Panel on Climate Change*. Cambridge University Press, Cambridge, UK.

IPCC 2014 *Climate Change 2014: Impacts, Adaptation, and Vulnerability. Contribution of Working Group II to the Fifth Assessment Report of the Intergovernmental Panel on Climate Change*. Cambridge University Press, Cambridge, UK.

Khodayar, S., Raff, F. & Kalthoff, N. 2015 Diagnostic study of a high precipitation event in the western Mediterranean region: adequacy of current operational networks. *Quarterly Journal of Royal Meteorological Society*. doi:10.1002/qj.2600.

Korichi, K., Hazzab, A. & Atallah, M. 2016 Flash floods risk analysis in ephemeral streams: a case study on Wadi Mekerra (northwestern Algeria). *Arabian Journal of Geosciences*. doi:10.1007/s12517-016-2624-2.

Koutsoyiannis, D. 2004 Statistics of extremes and estimation of extreme rainfall, 1, theoretical investigation. *Hydrological Sciences Journal* **49** (4), 575–590.

Koutsoyiannis, D. 2007 A critical review of probability of extreme rainfall: principles and models. In: *Advances in Urban Flood Management* (R. Ashley, S. Garvin, E. Pasche, A. Vassilopoulos & C. Zevenbergen, eds.). Taylor and Francis, London, pp. 139–166.

Lionello, P. & Scarascia, L. 2020 The relation of climate extremes with global warming in the Mediterranean region and its north versus south contrast. *Regional Environmental Change* **20** (1), 1–16.

Llasat Botija, M. D. C., Llasat-Botija, M., Prat Sabartés, M., Porcu, F., Price, C., Mugnai, A. & Yair, Y. 2010 High-impact floods and flash floods in Mediterranean countries: the FLASH preliminary database. *Advances in Geosciences* **23**, 47–55.

Lloyd-Hughes, B. & Saunders, M. A. 2002 A drought climatology for Europe. *International Journal of Climatology* **22**, 1571–1592.

Mandal, S. & Choudhury, B. U. 2015 Estimation and prediction of maximum daily rainfall at Sagar Island using best fit probability models. *Theoretical and Applied Climatology* **2015** (121), 87–97.

Salhi, C., Touaibia, B. & Zeroual, A. 2013 Les réseaux de neurones et la régression multiple en prédiction de l'érosion spécifique: cas du bassin hydrographique Algérois-Hodna-Soummam (Algérie)/Neural networks and multiple regression approaches in the prediction of specific erosion: case of the Algérois-Hodna-Soummam basin, Algeria. *Hydrological Sciences Journal* **58** (7), 1573–1580.

Şen, Z. 2020 *Earth Systems Data Processing and Visualization Using MALAB*. Springer-Nature, Switzerland, p. 277.

Şen, Z. & Eljadid, A. G. 1999 Rainfall distribution functions for Libya and rainfall prediction. *Hydrological Sciences Journal* **44**, 665–680.

Shabri, A. & Mohd Arif, N. 2009 Frequency analysis of maximum daily rainfalls via L-moment approach. *Journal Sains Malaysiana* **38** (2), 149–158.

Taibi, S, Meddi, M. & Gil, M. 2015 Evolution des pluies extrêmes dans le bassin du Chéliff (Algérie) au cours des 40 dernières années 1971–2010/Evolution of extreme rainfall in Cheliff basin (Algeria) over the past 40 years from 1971 to 2010. In: *Proceedings of the International Association of Hydrological Sciences*. Vol. 369, pp. 175–180.

Thom, H. C. S. 1958 A note on the gamma distribution. *Monthly Weather Review* **86**, 117–122.

Wilk, M. B., Gnanadesikan, R. & Huyett, M. J. 1962 Probability plots for the gamma distribution. *Technometrics* **4** (1), 1–20.

Zahar, Y. & Laborde, J.-P. 2007 'Modélisation statistique et synthèse cartographique des précipitations journalières extrêmes de tunisie'/Statistical modelling and cartography of extreme daily rainfall events in Tunisia. *Revue des Sciences de l'Eau* **20** (4), 409–424.

Zeggane, H. & Boutoutaou, D. 2017 Etude regionale des pluies maximales journalieres annuelles frequentielles du centre nord d'Algerie/A regional study to calculate daily maximum frequency precipitation in north-central Algeria. *Lebanese Science Journal* **18** (2), 166.

Zeroual, A., Assani, A. A., Meddi, M. & Alkama, R. 2019 Assessment of climate change in Algeria from 1951 to 2098 using the Köppen–Geiger climate classification scheme. *Climate Dynamics* **52** (1–2), 227–243.

First received 14 July 2020; accepted in revised form 6 November 2020. Available online 1 December 2020